

Available online at [www.sciencedirect.com](http://www.sciencedirect.com)**ScienceDirect**

Physics Procedia 69 (2015) 284 – 291

Physics

**Procedia**

10 World Conference on Neutron Radiography 5-10 October 2014

## Simulation of fast neutron radiography with a Time-of-Flight system

D. Chen<sup>a,b</sup>, J. Bao<sup>a\*</sup>, Q. Zhang<sup>a</sup>, S. Han<sup>b</sup>, J. Ren<sup>a</sup>, Y. Nie<sup>a</sup>, X. Ruan<sup>a</sup>, L. Hou<sup>a</sup><sup>a</sup>Science and Technology on Nuclear Data Laboratory, China Institute of Atomic Energy, Beijing, China, 102413<sup>b</sup>Neutron Scattering Laboratory, China Institute of Atomic Energy, Beijing, China, 102413

---

### Abstract

A novel fast neutron imaging method with Time-of-Flight was analyzed, which can provide a way to improve ratio of signal to noise for discrimination of scattered particles from the background, especially for bulky sample examination. For the same system spatial resolution, the length of each unit in scintillator detector array can be increased to improve detection efficiency, which is higher than for the traditional neutron image plate obviously. Key parameters such as detection efficiency and spatial resolution have been simulated by means of a Monte-Carlo method, and the ratio of signal to noise effect was estimated from MC and experimental results. Spatial resolution and contrast of compound sample have been calculated.

© 2015 The Authors. Published by Elsevier B.V. This is an open access article under the CC BY-NC-ND license (<http://creativecommons.org/licenses/by-nc-nd/4.0/>).

Selection and peer-review under responsibility of Paul Scherrer Institut

**Keywords:** Fast neutron radiography; Time-of-Flight; Scintillator detector array; Monte-Carlo method; SNR

---

### 1. Introduction

Due to good penetration of fast neutron through high-Z materials and large cross section of interaction, fast neutron radiography is believed to be capable of detecting structures in thick objects of large size. Thus, fast neutron radiography can be applied widely (Vontobel et al., 2004; Hall et al., 2006; Eberhardt et al., 2006; Allman et al., 2006; Hall et al., 2001; Mikerov et al., 2001). However, fast neutron radiography has not industrial standard. This is caused by two reasons as followed: the first one is the lack of transportable neutron sources with high flux

---

\* Corresponding author. Tel.: +00861069358640.

E-mail address: [baojie@ciae.ac.cn](mailto:baojie@ciae.ac.cn)

The project supported by National Science Foundation of China under Grant No. 11005157

and small spot size. Some labs (Hiraota et al., 2010; Zboray et al., 2011; Ludewigt et al., 2011) have developed compact neutron accelerator, but these were short of experimental support of fast neutron imaging; the second one is the lack of measurement methods of high spatial resolution and high detection efficiency combined with high ratio of signal to noise (SNR) for bulky sample examination. For decades, some groups have carried out investigations of fast neutron radiography and tried to resolve the latter (Yoshii et al., 1996; Ambrosi et al., 1998; Ambrosi et al., 1998). However, their results show that the best spatial resolution (Dangendorf et al., 2004; Dangendorf et al., 2006) of a scintillator detector is on the level of mm magnitude, and its detection efficiency is lower than 3%. The fixed spatial resolution is 10~100 $\mu$ m magnitude which based on GEM/MicroMegas detector, but its detection efficiency is lower than 0.1%.

In this paper, for the sake of measurement with high spatial resolution and detection efficiency combined with high ratio of signal to noise, a new scintillator detector array concept based on the Time-of-Flight (TOF) technique is presented for fast neutron imaging as a practical method. The neutron TOF method is a useful way for neutron energy spectrum measurement because of the better energy resolution compared to others, so it can effectively decrease background. In fast neutron imaging, the collimated mono-energy source neutron beam penetrates the bulky sample, some neutrons could be scattered by the sample, whereby their energies can decrease. The TOF method can discriminate these scattered neutrons from mono-energy source neutrons. As shown in table 1, SNR is defined as the ratio of 14MeV source neutrons to scattered neutrons for different thicknesses in polyethylene and iron samples. The result was obtained from MCNP simulations.

Table 1. Ratio of 14MeV source neutrons/scattered neutrons for different thicknesses

thickness	0cm	5cm	10cm
Polyethylene	16.79	9.77	6.11
Iron	16.79	4.65	1.77

When the sample doesn't exist (the thickness of sample is 0 cm), SNR is about 16.79 which means 5.6% (1/16.79) neutrons were scattered by air in the MCNP model. If the thickness of a polyethylene sample is 10 cm, SNR is about 6.11 which means 14.1% (1/6.11) neutrons were scattered by air and polyethylene. If the thickness of an iron sample is 10 cm, SNR is about 1.77 which means 56.5% neutrons were scattered by air and iron. Obviously the sample is thicker, the noise is higher. Neutron TOF method can select source neutron signal for image.

In the following sections, principle of the scintillating detector array, TOF method and simulation of detector character are introduced respectively.

## 2. Detector description & arrangement

Fig. 1 shows the experimental arrangement of fast neutron radiography with scintillator detector array based on the TOF method. Our experiment has a long flight path (approximately 6 m), which can be used to decrease the background of neutrons scattered by the samples.  $L/D=600$  means approximately parallel neutron beam at the sample position. Such an experimental arrangement is a good solution to decrease geometric uncertainty. In the end, different magnification ratios and mm magnitude spatial resolutions can be realized by changing the distance from neutron source to sample combined in the experimental arrangement. Here the scintillation detector array consists of  $16 \times 16 = 256$  units and each independent scintillator unit is a  $3\text{mm} \times 3\text{mm} \times 100\text{mm}$  plastic scintillator of BC400 type which is based on polyvinyltoluene covered with an aluminium film thickness of 2  $\mu\text{m}$ . This geometric design is enough to avoid the effect of crosstalk for recoiled protons which are generated by 14MeV neutrons. Each scintillator couples to a unit of position sensitive PMT (PSPMT) unit respectively, which can generate an anode signal as the stop signal of the TOF method, the corresponding start signal is the pulsed pick-up signal from the accelerator. The position sensitive PMT is an Hamamatsu H9500 type, which has an  $16 \times 16$  multi-anode and fast time response. Each independent scintillator with aluminium film has a high detection efficiency and different units have no photon crosstalk (see Fig. 2).

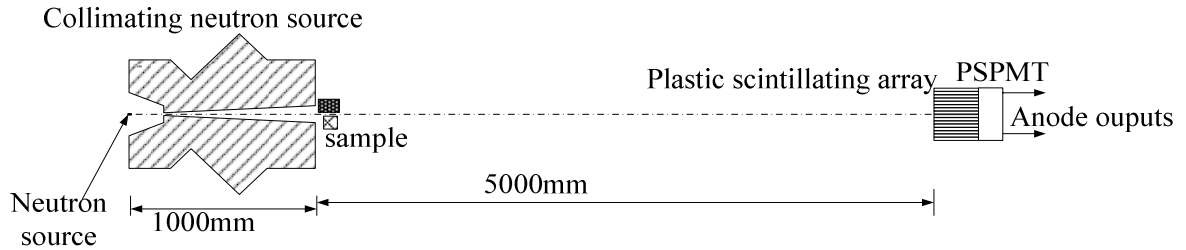


Fig.1 Scheme of experiment arrangement, where the distance from the pulsed neutron source to scintillating detector array L is 6000 mm, and the smallest diameter of collimator D is 10mm.

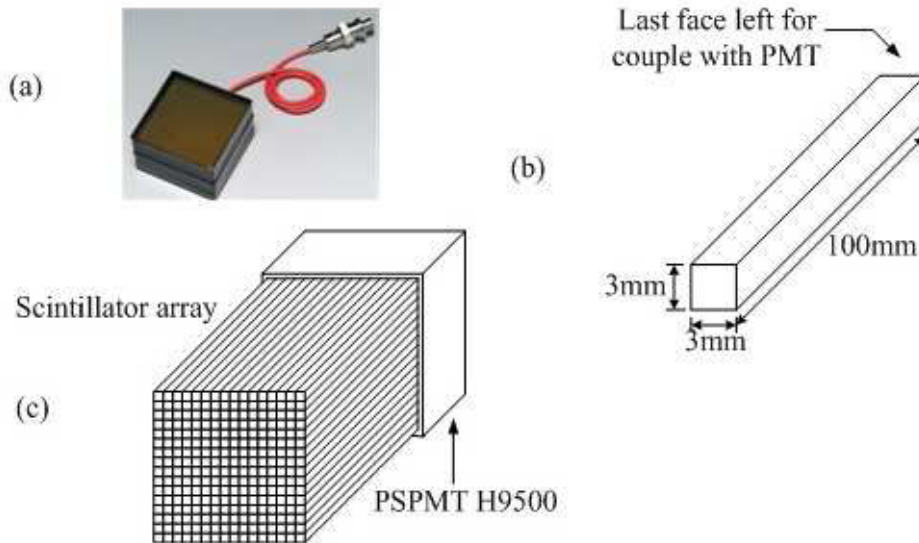


Fig.2 Plastic scintillator array scheme. (a) photo of Hamamatsu H9500 PSPMT and its number definition of each unit; (b) geometry of plastic fibre, 5 faces were covered with 2  $\mu\text{m}$  aluminium film, the end face(3mm  $\times$  3mm) was left for coupling with PMT; (c) all 16  $\times$  16 fibres coupled to the H9500 as a detector array.

The 600kV Cockcroft-Walton accelerator constructed at CIAE could provide  $\sim 10^{10}/\text{s}$  pulsed neutrons with 14MeV with the frequency of 1.5MHz and a pulse width of about 2~3 ns. 14MeV neutrons were produced by the  $T(d,n)\alpha$  reaction. The target is solid tritium in titanium metal on a molybdenum pad. The tritium density is above 1mg/cm<sup>2</sup>. The diameter of the neutron source spot is 3~5 mm. The deuterium beam current can attain 30 $\mu\text{A}$  under pulsed mode so that the corresponding neutron yield is about  $8 \times 10^9/\text{s}$ .

Figure3 shows the design of the readout electric circuit. Each unit can generate a fast signal from corresponding anode when neutron collides with detector. The discriminator can generate a time signal to discriminate neutron signal whether directly come from DT target or scattering neutron. There are two outputs, one for the address encoder and its register, the other for an "OR" logical unit as TOF start signal. TOF stop signal comes from delayed pulsed signal of accelerator. The result is the corresponding address number add 1 because the TDC generates one effective TOF count in the DAQ.

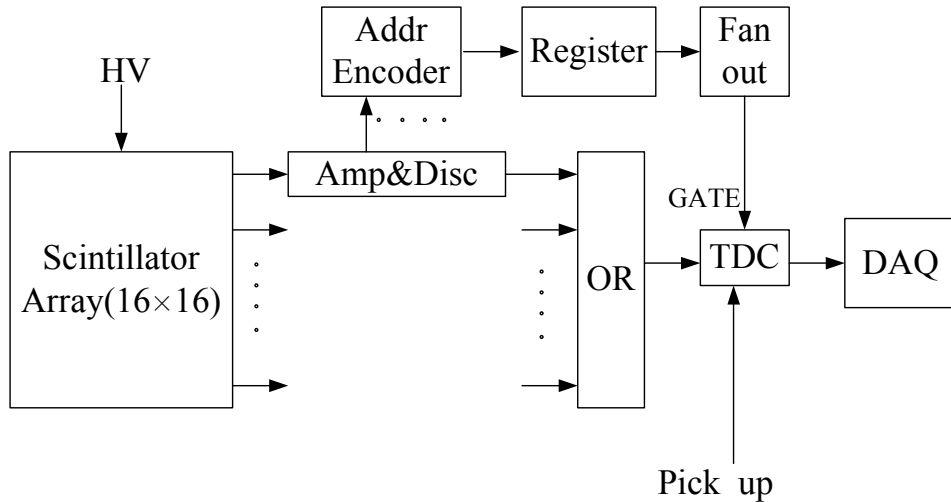


Fig.3 Readout electric circuit diagram  
TDC: Time-to-Digital Converter; DAQ: Data Acquisition

Figure 4 shows a typical TOF spectrum of DT neutron source measured directly by a liquid scintillation detector. The gamma peak and neutron peak can be obviously discriminated from TOF spectrum. Because source neutrons with 14MeV are only present in neutron peak and the scattered neutrons are distributed over the flat region, the background of scattered neutron can be reduced by TOF method. Considering the considerable flight distance and shielding effect, the uncertainty of background reduction can be controlled below 1% when the density of sample is about 50g/cm<sup>2</sup>. The SNR can be changed from about 100:50 to 100:1.

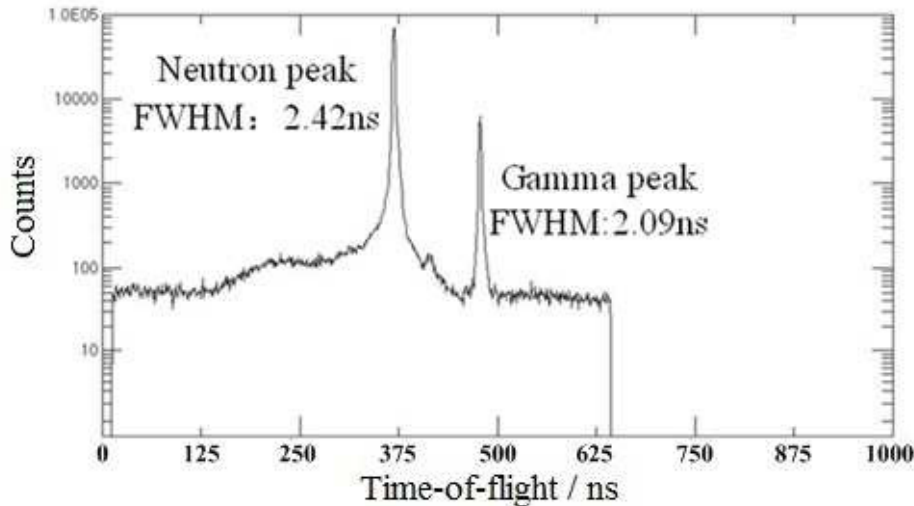


Fig.4 A typical Time-of-Flight spectrum measured directly from the liquid scintillator of the pulsed DT source where the FWHM of the neutron peak and gamma peak are 2.42 ns and 2.09 ns, respectively.

The count rate depends on the length from neutron source to detector and the detection efficiency. For a better energy resolution of the neutron TOF spectrum and for a high SNR, a long path is required. In table 1, the SNR of neutrons through an iron sample of 10cm thickness is about 1.77, which means source neutrons is 1.77 times of scattered neutrons. The scattered neutrons are dispersed in left of neutron peak because of lower energy.

The neutron flight path is 6m and the detector thickness is 100 mm, then the intrinsic efficiency at the threshold above 2MeV is 20% for the case of 14MeV incident neutrons. When the source neutron yield is  $\sim 1010/s$ , the count rate of each unit is about 40Hz. If the measuring time is 20s, the count is 800 and the statistical deviation is about 3.5% for the sake of high SNR.

### 3. Spatial resolution and contrast of detector

The lengths from sample and scintillating detectors to the neutron source are 1m and 6m respectively. Thus, the magnification ratio is about 6. In the simulation, the first sample is made of iron and its thickness is 50 mm. There is a structure flaw of  $30\text{mm} \times \Phi 1\text{mm}$  in the sample used in simulation. The simulation result in such a geometric arrangement is given in Fig. 5. It is shown that 1 mm spatial resolution can be obtained. The minimum spatial resolution is about 0.5 mm under considering the count rate and each unit dimension of about 3 mm.

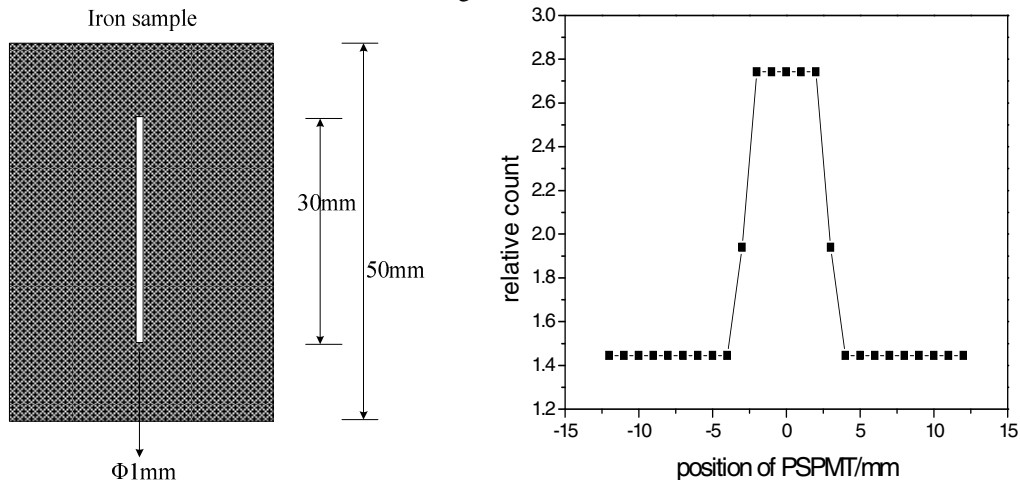


Fig.5 Magnification factor for the experimental arrangement where the lengths from sample and scintillating detectors to neutron source are 1m and 6m, respectively and sample has a structure flaw of  $\Phi 30\text{mm} \times \Phi 1\text{mm}$  from MCNP simulations.

The detection efficiency is also an important factor for fast neutron imaging and will determine the measuring time. Assuming that each “pixel” is an independent unit and has no optical and recoiled proton crosstalk, a very high efficiency can be theoretically obtained when increasing the length of scintillator. We performed the simulation of detection efficiency of the scintillator with varying length by using NEFF program from PTB (Physikalisch-Technische Bundesanstalt). The detection efficiency simulation results are shown in Fig. 6. The longer the scintillator is, the larger is the efficiency of each unit.

The neutron multi-scattering effect has been also simulated by MCNP. It depends on the length of the scintillator, as shown in Table2. The point neutron source emits in one direction only to one fibre directly. Neutron can impinge on that fibre only, or multi-scatter in other 255 fibres. There is a higher SNR for short scintillators with low efficiency. As the length increases, the SNR decreases but smoothes out gradually to 20cm about  $\text{SNR}=4.2$ . This means that there are about 23.8% ( $1/4.2$ ) is multi-scattered neutrons in the TOF spectra. Multi-scattering happened in the detector array, so it cannot be eliminated by the TOF method. Considering 5% of statistical error with background of 19% multi-scattered neutron all from detector neutron cross talk, 800 counts are needed in each unit which means about 20s measuring time under 1010/s of neutron source yield.

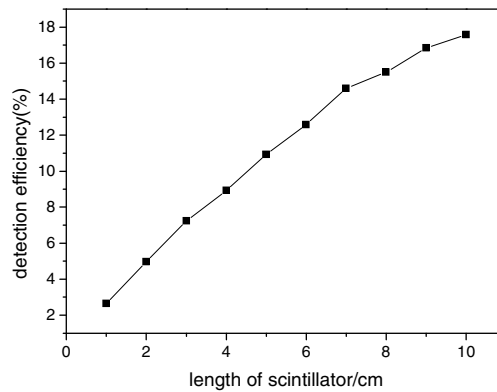


Fig.6 The simulation for detection efficiency corresponding to scintillator with various length

Table 2. The simulation of neutron multi-scattering in scintillators with various lengths

Length of scintillator/cm	1	2	3	4	5	6
SNR	14.25	9.52	7.78	6.85	6.16	5.61
Length of scintillator/cm	7	8	9	10	15	20
SNR	5.26	4.91	4.77	4.66	4.40	4.20

In order to further verify the feasibility of this experimental set-up, we have used MCNP to simulate images of the second sample. As shown in Fig. 7(a), the second sample was designed with two materials of iron and polyethylene.

Different materials and a distinct stepwise structure of the sample are used for comparison of contrast. The width of the stepwise structure can reflect the minimum spatial resolution. Here it is 1mm width in the sample. There is a  $16 \times 16$  units plastic scintillator array 6 meters away from neutron source. Each unit geometry is  $3\text{mm} \times 3\text{mm}$ , 6mm length will cause 2~3 units response. Each unit will be defined as one detector for MCNP simulation. For the system can select source neutron by neutron TOF method, the scattering part will be discriminated in MCNP result which can reflect the real neutron TOF experimental process. Fig.7(b) gives the simulated two dimensional image result from MCNP. The sample is shown in fig.7(a). We can see that the counts in the longest step position is lowest due to the least probability of neutron transmission shown in A-B of fig.7(b), the counts in the shortest step position is high due to the highest probability of neutron transmission to iron shown in C-D of fig.7(b), the counts in the position of polyethylene is higher due to higher probability of neutron transmission to polyethylene compared with iron shown in E-F of fig.7(b), the counts in the position of no sample is the highest due to neutron direct transmission to sample. So the two dimensional image simulation result can correctly express the structure of sample designed. From Fig.7, we can also see that 1cm contrast sensitivity and 1mm material width can be obtained. It is required to shrink the size of each detector unit or increase length of neutron flight to acquire higher spatial resolution.

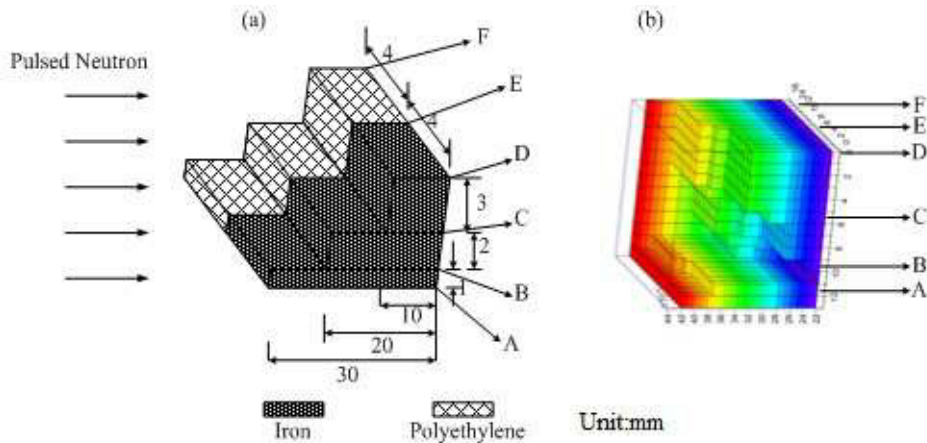


Fig.7 (a) Stepwise structure of sample made of iron and polyethylene where the longest step is 30mm and the shortest step is 10mm;(b) two dimensional image simulation result from MCNP where the highest counts correspond to hollow parts in the sample and the lowest counts correspond to the longest step parts.

#### 4. Summary and conclusion

The performance of a scintillating detector array based on the TOF method was analyzed using Monte-Carlo methods. The simulation results show that fast neutron radiography with a scintillating detector array based on Time-of-Flight method can raise the SNR greatly from 100:50 to 100:1 for a bulky sample, obtain spatial resolution of mm even sub-mm magnitude and high detection efficiencies of over 10%. The neutrons can directly be measured by the scintillating detector array, and higher detection efficiency can be obtained than that of case of neutron converter+CCD design because of the PSPMT structure in detectors. About 20 seconds of scan time for one area measurement is enough to determine whether there is a flaw in a sample under 1010/s pulsed neutrons yield or not. It is a speedy method of fast neutron radiography. The method will be well suited to non-destructive examination of known structure sample with unknown interior defects.

#### Acknowledgement:

Authors acknowledge Professor Tang Hongqing and Professor Zhou Zuying from China Institute of Atomic Energy, and Professor Sakurai from Tokyo University for their help in designing this new method.

#### Reference:

- P. Vontobel, E. Lehmann, G. Frei, Neutrons for the study of adhesive connections, 16th World Conference on Nondestructive Testing (2004).
- J. Hall, B. Rusnak, P. Fitsos, High energy neutron imaging development at LLNL, UCRL-CONF-230835 (2006).
- J. E. Eberhardt, Y. Liu, S. Rainey, G. J. Roach, R. J. Stevens, B. D. Sowerby, J. R. Tickner, Fast neutron and gamma ray interrogation of air cargo containers, Proceedings of Science, International Workshop on Fast Neutron Detectors (2006).
- B. E. Allman, K. A. Nugent, Phase imaging with thermal neutrons, Phys.B 385 (2006) 1395.
- J. Hall, F. Dietrich, C. Logan, B. Rusnak, Recent results in the development of fast neutron imaging techniques, AIP Conference Proceedings 576 (2001) 1113.
- V. Mikerov, I. Zhitnik, J. Barmakov, E. Bogolubov, V. Ryzhkov, A. Koshelev, N. Soshin, W. Waschkowski, R. Lanza, Prospects for efficient detectors for fast neutron imaging, Appl.Radi.Isot. 61 (2004) 529.
- K. Hiraota, A plan for compact accelerator-based neutron source and detector systems at RIKEN, UCANS-1, Beijing (2010).
- R. Zboray, R. Adams, M. Cortesi, Development of a compact DD neutron generator with a small emitting spot for fast neutron imaging, The 2nd International Workshop on Fast Neutron Detectors and Applications (2011).
- B. Ludewigt, Neutron source R&D-from compact generators to neutron beams, The 2nd International Workshop on Fast Neutron Detectors and Applications (2011).

- K. Yoshii, H. Kobayashi, Correction of fast neutron scattered components from fast neutron radiography images, *Nucl.Instr.&Meth. A* 377 (1996) 76.
- R. M. Ambrosi, J. I. W. Watterson, Factors affecting image formation in accelerator-based fast neutron radiography, *Nucl.Instr.&Meth. B* 139 (1998) 279.
- R. M. Ambrosi, J. I. W. Watterson, B. R. K. Kala, A Monte Carlo study of the effect of neutron scattering in a fast neutron radiography facility, *Nucl.Instr.&Meth. B* 139 (1998) 286.
- V. Dangendorf, A. Breskin, R. Chechik, G. Feldman, M. B. Goldberg, O. Jagutzki, C. Kersten, G. Laczko, I. Mor, U. Spillman, D. Vartsky, Detectors for energy-resolved fast neutron imaging, *Nucl.Instr.&Meth. A* 535 (2004) 93.
- V. Dangendorf, R. Lauck, F. Kaufmann, J. Barnstedt, A. Breskin, O. Jagutzki, M. Kremer, D. Vartsky, Time-resolved fast neutron imaging with a pulse counting image intensifier, *International Workshop on Fast Neutron Detectors and Applications* (2006).
- BC400 premium plastic scintillator, <http://www.detectors.saint-gobain.com>.
- Hamamatsu flat panel type multianode photomultiplier tube assembly H9500, <http://www.hamamatsu.com>.